Journal of the Earth and Space Physics
Homepage: https://jesphys.ut.ac.ir
Vol. 51, No. 4, Winter 2026, P. 29-44
(Research Article)

Statistical Assessment of Magnetic Precursors to the April 1, 2014 Chile 8.2 Earthquake Using Swarm Satellite Data

Pourbeyranvand, Sh.[1] ✉ | Firouzian, A. H.[1]

1. Department of Seismological Research Center-Seismology, International Institute of Earthquake Engineering and Seismology, Tehran, Iran.

Corresponding Author E-mail: beyranvand@iiees.ac.ir

(Received: 16 Aug 2025, Revised: 14 Oct 2025, Accepted: 30 Dec 2025, Published online: 17 March 2026)

Abstract

Satellite-based monitoring of geomagnetic field variations offers a promising avenue for identifying earthquake precursors. The use of satellite data to detect such anomalies has garnered significant attention, given its global coverage and independence from ground-based limitations. In this study, we applied the characteristic curve method to Swarm satellite magnetic data to investigate pre-seismic anomalies preceding the Mw 8.2 Chile earthquake on April 1, 2014. After subtracting the International Geomagnetic Reference Field (IGRF-14), we identified a statistically significant anomaly in the northward magnetic component (BN) approximately 33 days before the event. The characteristic curve method, which is based on plotting the satellite data over the study area repeatedly on consecutive orbits, enabled quantification of this deviation, revealing a statistically significant signal while accounting for natural geomagnetic variability. Graphical analysis of the data highlighted this anomaly as a pronounced feature, distinguishable from typical fluctuations. This anomaly exceeded ±20 nT uncertainty bounds and persisted across multiple orbits. To validate its uniqueness, we analyzed two control intervals, three months before and after the study window, using the same method, confirming that no comparable anomalies occurred outside the precursor period. The anomaly's directional specificity, temporal isolation, and amplitude support its interpretation as a genuine pre-seismic signal, likely linked to lithosphere-atmosphere-ionosphere coupling processes. These findings demonstrate the robustness of the characteristic curve method for satellite data and reinforce the potential of Swarm observations in short-term earthquake forecasting.

Keywords: Characteristic curve method, Chile earthquake, Geomagnetic anomaly, Precursor detection, SWARM satellite.

1. Introduction

Since ancient times, humans have sought ways to predict earthquakes due to the dangers they pose. Despite extensive efforts, challenges and skepticism persist regarding the feasibility of accurate earthquake prediction (Richter, 1958). However, recent advances in remote sensing technologies and geophysical data analysis have renewed hope in this field. The European Space Agency (ESA), through its SWARM mission, has provided a platform for studying Earth's magnetic field and investigating geomagnetic precursors.

Using ground-based stations to detect magnetic anomalies before earthquakes is a common approach in seismological studies. However, due to the limited global distribution of magnetometer stations, satellite data, particularly from the SWARM mission, offer a valuable alternative for global-scale analysis. Studies on earthquakes in Nepal, Ecuador, and Mexico have shown that variations in magnetic field components and ionospheric conditions may serve as seismic precursors (De Santis et al., 2017; Akhoondzadeh et al., 2018; Zhu et al., 2019).

To identify anomalies in SWARM data, various tools and algorithms have been developed. These include statistical methods such as Principal Component Analysis (PCA) and General Empirical Orthogonal Functions (GEOF), which have been applied in studies like Pavlovic et al. (2021). Additionally, algorithms for noise reduction and the extraction of pre-seismic signals have been designed (Ghamry et al., 2021; Christodoulou et al., 2019). Repeated studies on specific earthquakes have further

Cite this article: Pourbeyranvand, Sh., & Firouzian, A. H., (2026). Statistical Assessment of Magnetic Precursors to the April 1, 2014 Chile 8.2 Earthquake Using Swarm Satellite Data. *Journal of the Earth and Space Physics*, 51(4), 29-44. DOI: http//doi.org/10.22059/jesphys.2025.400455.1007714

E-mail: (1) ah.firouzian@stu.iiees.ac.ir

Publisher: University of Tehran Press.
DOI: http//doi.org/10.22059/jesphys.2025.400455.1007714
Print ISSN: 2538-371X
Online ISSN: 2538-3906

validated these methods (De Santis et al., 2019).

Recent advancements in satellite-based geophysical monitoring have significantly enhanced our understanding of seismo-magnetic anomalies as potential earthquake precursors. Akhoondzadeh et al. (2022) developed a deep learning framework using Swarm satellite data to detect anomalies in the magnetic field, electron density, and temperature preceding the 2021 Mw 7.1 Japan earthquake, demonstrating the utility of multi-parameter spaceborne observations. Similarly, Liu et al. (2024) analyzed ionospheric and magnetic storm disturbances via the China Seismo-Electromagnetic Satellite (CSES), revealing spatial correlations with seismic activity in August 2018. Akhoondzadeh (2025) further explored the predictive capacity of lithosphere-atmosphere-ionosphere coupling anomalies using satellite-derived data, proposing a methodology for estimating earthquake magnitude and timing. Complementing these efforts, Conti et al. (2021) provided a comprehensive review of ground-based precursor observations, contextualized alongside satellite-based findings in a companion article, while Hegy (2025) synthesized Swarm mission data to identify magnetic field perturbations linked to tectonic stress accumulation. Collectively, these studies underscore the growing reliability and resolution of satellite platforms in capturing electromagnetic precursors, offering promising avenues for earthquake forecasting and hazard mitigation.

2. Parameters Influencing Magnetic Field Changes in Earthquake Detection

Magnetic field fluctuations observed prior to seismic events are influenced by a range of geophysical and environmental parameters. Understanding these factors is essential for distinguishing genuine earthquake precursors from background geomagnetic variability. One of the primary contributors is tectonic stress accumulation in the lithosphere. As stress builds along fault zones, it can induce physical processes such as microfracturing and fluid migration, which generate electric currents through electrokinetic effects. These currents produce magnetic field perturbations that may be detectable at the surface or by satellites (Fenoglio et al., 1995). Additionally, the piezomagnetic effect—where stress alters the magnetization of ferromagnetic minerals—can lead to measurable magnetic anomalies (Sasai, 1991).

Another significant factor is the emission of geochemical gases, particularly radon. Elevated radon levels prior to earthquakes have been linked to increased atmospheric ionization, which modifies the conductivity of the lower atmosphere and can influence the coupling between the lithosphere and ionosphere. This coupling, described within the Lithosphere–Atmosphere–Ionosphere Coupling (LAIC) framework, provides a pathway for stress-induced changes in the lithosphere to manifest as ionospheric and magnetic anomalies (Pulinets & Ouzounov, 2011). Ionospheric conditions themselves play a critical role. Parameters such as total electron content (TEC), electron density, and ionospheric current systems (e.g., the equatorial electrojet) can modulate the magnetic field, especially in low-latitude regions where diurnal and seasonal variations are pronounced. High-latitude regions, by contrast, are dominated by auroral currents and solar wind interactions, which introduce significant noise and complicate precursor detection. Consequently, mid-latitude zones are often preferred for magnetic precursor studies due to their relative geomagnetic stability (Conti, Picozza, & Sotgiu, 2021).

External geomagnetic disturbances, such as geomagnetic storms and solar flares, also affect magnetic field measurements. These space weather events can produce transient anomalies that mimic or obscure seismic-related signals, necessitating careful filtering using models like the International Geomagnetic Reference Field (IGRF) (European Space Agency, 2019). Finally, the quality and configuration of satellite instrumentation influence detection capabilities. For instance, the Swarm mission's Vector Field Magnetometer (VFM) and Absolute Scalar Magnetometer (ASM) provide high-resolution measurements of magnetic field components, enabling detailed analysis of directional anomalies (Friis-Christensen et al., 2006). Data preprocessing techniques, such as the characteristic curve method, further enhance signal discrimination by establishing statistical envelopes of normal behavior and flagging

deviations as potential precursors (De Santis et al., 2019).

3. Data and method

The European Space Agency's Swarm mission comprises three satellites equipped with instruments capable of measuring both vector and scalar components of Earth's magnetic field. Each satellite carries two distinct magnetometers: the Vector Field Magnetometer (VFM), which records the direction of the magnetic field, and the Absolute Scalar Magnetometer (ASM), which measures its intensity. These instruments are mounted on a boom to minimize magnetic interference from the spacecraft body (Friis-Christensen et al., 2006; Léger et al., 2015).

The ASM operates based on the Electron Spin Resonance (ESR) principle, utilizing the Zeeman Effect to determine magnetic field strength with high precision. However, the ASM onboard Swarm-C experienced a malfunction on November 5, 2014, which has limited its scalar data availability since that date (European Space Agency, n.d.; Jackson, 2015).

For scientific analysis, one of the primary data products used is the MAGx_LR_1B catalog. This Level 1b product provides synchronized vector and scalar magnetic field measurements at a sampling rate of 1 Hz. The data are interpolated to exact UTC seconds, allowing for continuity even in the presence of minor gaps in raw measurements. Interpolation procedures are documented in the ESA's processor algorithm documentation (European Space Agency, 2019).

The MAGx_LR_1B product includes:

- Magnetic field intensity (F) from ASM
- Magnetic field vector (B) from VFM
- Error estimates and stray field corrections (e.g., sun-induced perturbations)
- Flags indicating data quality and instrument status

These datasets are essential for identifying geomagnetic anomalies and potential earthquake precursors, especially when combined with ionospheric and ground-based observations.

The approach applied in this study, referred to as the "characteristic curve" method, has traditionally been employed at ground-based stations (see Taherinya and Pourbeyranvand, 2021), but to date, it has not been utilized for satellite magnetic data analysis. For satellite data acquisition, the VirES platform was used, offering tailored access to Swarm mission data. This service allows users to specify parameters such as satellite catalog, temporal intervals, and geographic scope. Notably, it can also generate values from the International Geomagnetic Reference Field (IGRF-14) for satellite positions (International Association of Geomagnetism and Aeronomy, 2024).

Magnetic field observations from the Swarm satellites corresponding to the 2014-04-01 Mw 8.0 earthquake in Chile (23:46 UTC) were downloaded for a 5-degree latitude and longitude window around the epicentral region. This geographic extent was chosen based on the Dobrovolsky radius (Dobrovolsky et al., 1977), which approximates the influence zone of an Mw 8.0 earthquake. The dataset was filtered to isolate measurements from Swarm-A (Figure 2). As a reminder, strain radius can be determined using the Dobrovolsky equation (Equation 1):

$$\rho = 10^{0.43M} \quad (1)$$

where M is the magnitude. It is assumed that almost all earthquake precursors are likely to fall within this circle. ρ represents the strain radius, which is the estimated radius around the epicenter within which earthquake precursors are most likely to occur. The unit of ρ is kilometers.

Following preprocessing, the intrinsic behavior of the data was characterized using a sliding window analysis across geographic latitudes. The methodology proceeded as follows:

- A window was defined to traverse the data longitudinally along latitude.
- Data points within the window were selected.
- The mean latitude of the data within the window was calculated.
- The median magnetic field value (B_median) was computed.
- The standard deviation (σ) of the magnetic field was determined.
- The window was shifted by its length and the process was repeated from Step 2 until the full latitudinal extent was covered.

Using this technique, each window yielded a trio of statistical descriptors: mean

latitude, median magnetic field strength, and standard deviation. Two envelopes $f(Lat_{mean}) = B_{median} + \sigma$ and $g(Lat_{mean}) = B_{median} - \sigma$ were plotted to define the characteristic range of "normal" magnetic field behavior along the latitudinal profile (Figure 3). Data points falling outside this envelope were flagged as anomalous.

The advantage of subtracting the IGRF model before generating the characteristic curve lies in its temporal invariance; as the IGRF does not account for short-term temporal variations, it serves as a robust baseline. Thus, any deviation from the expected magnetic behavior within the characteristic envelope is presumed to represent genuine anomalies rather than noise, enhancing the method's reliability in identifying pre-seismic magnetic irregularities.

The Earth's geomagnetic field exhibits distinct latitudinal characteristics that influence its suitability for earthquake precursor detection. High-latitude regions are subject to intense magnetospheric disturbances caused by solar wind interactions and auroral currents, while low-latitude regions are dominated by equatorial electrojets and strong diurnal ionospheric variability. Satellite missions such as Swarm capture these dynamics globally, but the data from these zones are often excluded from pre-seismic studies due to the dominance of non-tectonic signals. By contrast, mid-latitude regions offer comparatively quiet geomagnetic environments, enabling clearer identification of subtle lithospheric-ionospheric coupling potentially linked to seismic activity.

Figure 1 displays residual magnetic field values B (N) relative to the IGRF model across latitudes. A concentrated and symmetrical distribution of data is observed at mid-latitudes, reflecting geomagnetic stability ideal for earthquake precursor analysis. In contrast, the wide scatter and asymmetry at high latitudes indicate significant magnetospheric noise from auroral activity, while disturbances at low latitudes suggest interference from equatorial electrodynamics. These fluctuations visually justify the exclusion of polar and equatorial data zones in seismic precursor research.

Figure 2 presents three-directional components of the geomagnetic field: northward (B Val N, blue), eastward (B Val E, red), and vertical (B Val C, green), recorded by the Swarm satellite. Each subplot illustrates temporal or spatial fluctuations in magnetic intensity, showing how the field varies with respect to Earth's surface and satellite trajectory. The contrast in patterns across these components reflects different geophysical sources and helps distinguish local magnetic features from broader ionospheric or lithospheric signals.

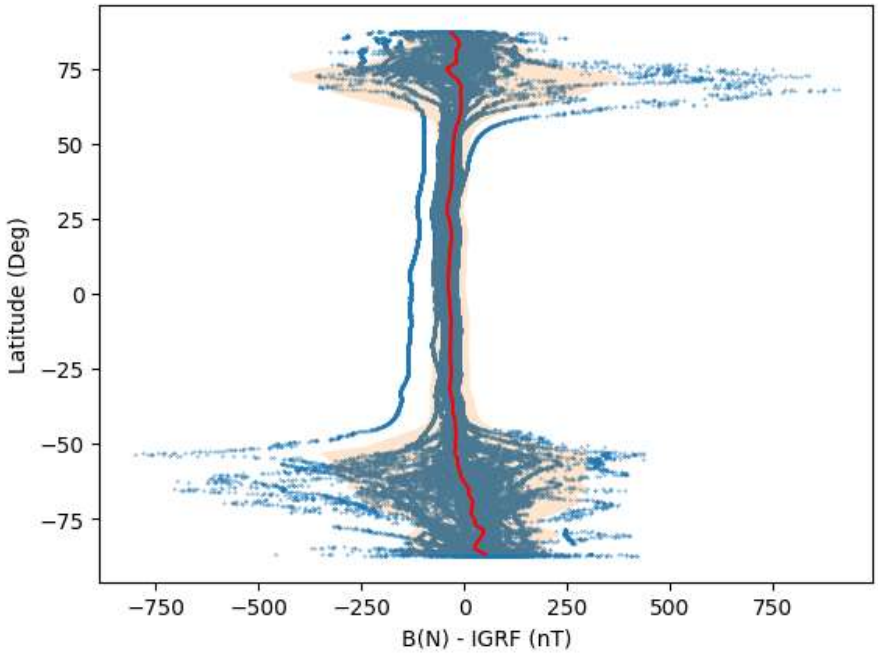

Figure 1. Latitudinal variation of geomagnetic field residuals from satellite observations, highlighting stable mid-latitude conditions versus noisy high and low latitudes influenced by auroral and equatorial currents.

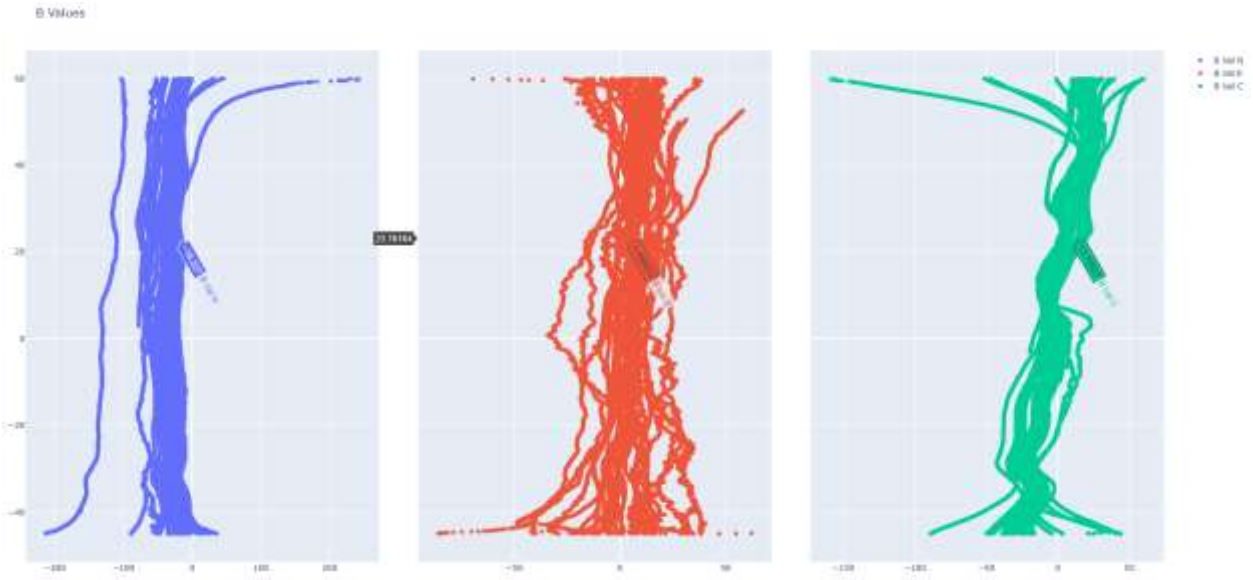

Figure 2. Directional components of the geomagnetic field (B Val N, B Val E, B Val C) captured by the Swarm satellite, highlighting spatial variability essential for isolating lithospheric signals in earthquake precursor studies.

Figure 3 illustrates the application of the characteristic curve method to Swarm satellite magnetic field data in the context of earthquake precursor analysis. The plot represents the relationship between the northward magnetic component (B_Val_N) and geographic latitude. The color gradient encodes the number of days before the earthquake, covering a 35-day period that includes the key anomaly window. A pronounced anomaly is observed at day -33 (dark blue curve separated on the left), suggesting a potential precursor signature. Notably, the curve associated with day -33 exhibits a distinct deviation from the surrounding data, suggesting a potential ionospheric or magnetospheric anomaly linked to earthquake preparation processes. This anomaly supports the hypothesis that lithosphere–atmosphere–ionosphere coupling mechanisms may manifest in magnetic field variations detectable by low-Earth orbit satellites. The characteristic curve method enables temporal tracking of such anomalies, offering a promising approach for short-term earthquake forecasting.

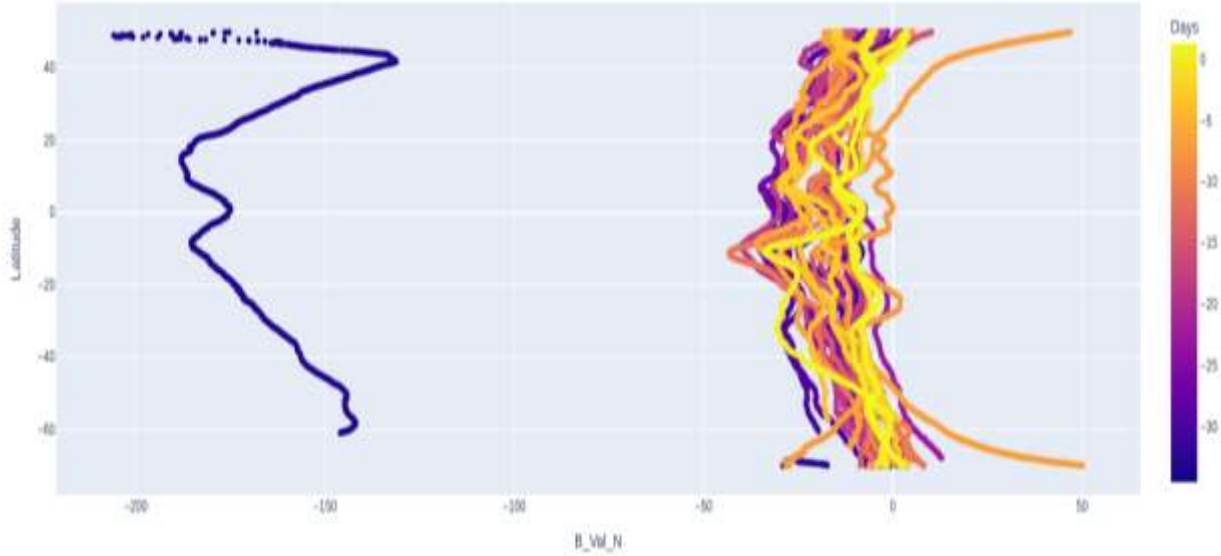

Figure 3. Application of the characteristic curve method to Swarm satellite magnetic data for earthquake precursor detection.

In Figure 4, the graph plots the same data, i.e., the deviation of the northward magnetic component (B(N) – IGRF) against geographic latitude over a temporal window spanning from 2014-02-15 to 2014-03-04, and it shows the same result. In addition, a light orange shaded region denotes the ±2σ uncertainty bounds, calculated to assess the statistical significance of observed anomalies.

In this figure, the characteristic curve plot displays multiple blue curves representing daily magnetic profiles, with a red line indicating the mean trajectory. A distinct deviation from the mean curve is observed on day -33 before the earthquake, exceeding the 2σ threshold and suggesting a statistically significant anomaly as seen before in Figure 3. This anomaly may reflect ionospheric or magnetospheric perturbations associated with lithospheric stress accumulation. The characteristic curve method enables temporal tracking of such anomalies, offering a robust approach for identifying short-term precursory signals in geomagnetic data.

4. Results

During the observational period from 15 February to 1 April 2014, which encompassed the lead-up to the Mw 8.0 Chile earthquake on 1 April 2014, a distinct anomaly in the magnetic field was identified within the satellite data. This anomaly was detected specifically on 27 February 2014, approximately 33 days before the main seismic event.

The anomaly was characterized by a significant deviation from the baseline magnetic behavior, as defined by the characteristic curve method applied to the Swarm-A satellite data. After subtracting the IGRF-14 geomagnetic model from the raw magnetic field observations, the remaining data were statistically assessed for irregularities. Using the sliding window algorithm described in the methodology, the anomaly was registered as a substantial outlier, falling outside the constructed envelope representing the normal geomagnetic variation range.

Figure 5 demonstrates the application of the characteristic curve method to Swarm satellite magnetic field data for earthquake precursor analysis. The figure comprises three plots corresponding to the northward (BN), eastward (BE), and vertical (BC) magnetic components, each plotted as the deviation from the International Geomagnetic Reference Field (IGRF) against geographic latitude. A fourth panel displays the geographic region of interest, covering parts of North and South America, including Chile, and the star represents the earthquake location.

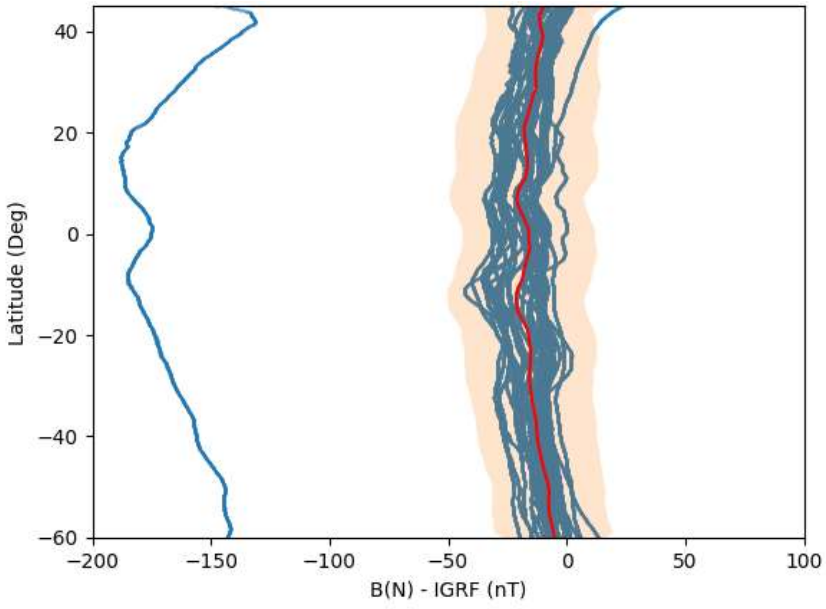

Figure 4. Characteristic curve analysis of Swarm satellite magnetic data for earthquake precursor detection with error band or uncertainty limits. The plot shows B(N) – IGRF versus latitude from 2014-02-15 to 2014-03-04. Blue lines represent daily magnetic profiles; the red line indicates the mean curve. The shaded orange band marks the ±2σ uncertainty range. A pronounced anomaly on day -33 exceeds the 2σ threshold, suggesting a potential precursor signal.

Each magnetic component plot includes multicolored curves representing daily measurements spanning ±40 days relative to the earthquake event. As before, the color gradient encodes temporal proximity to the earthquake, with day -33 highlighted within the spectrum. Shaded bands around the curves denote ±2σ uncertainty limits, allowing for statistical assessment of deviations.

A distinct anomaly, which was shown on Figures 2 and 3, is observed in the BN component on day -33, where the curve deviates significantly beyond the 2σ bounds. This anomaly is weakly mirrored in the BE or BC components, suggesting directional specificity in the magnetic perturbation. The absence of corresponding anomalies in the other components strengthens the interpretation that the BN deviation may reflect a localized ionospheric or magnetospheric disturbance associated with lithospheric stress accumulation. These findings support the utility of the characteristic curve method in isolating component-specific precursory signals.

The anomaly's persistence and amplitude suggest a non-random magnetic perturbation that may correspond to pre-seismic lithospheric or ionospheric processes. Notably, no similar anomalies were observed in adjacent time windows, reinforcing the uniqueness of this signal within the studied interval. These results support the hypothesis that satellite-based magnetic observations, when properly filtered and benchmarked against time-invariant models, may yield valuable precursors for seismic activity studies. The detection of this anomaly presents a compelling case for further investigation into the role of geomagnetic fluctuations in earthquake forecasting frameworks.

The statistical significance of the detected anomaly was assessed using a sliding window approach that generated median and standard deviation envelopes across latitudinal profiles. Specifically, the characteristic curve method defines a "normal" magnetic behavior envelope as Bmedian ±σB, where σ is the standard deviation of the magnetic field within each latitudinal window. Data points falling outside this envelope are flagged as anomalous. To ensure robustness, the anomaly observed on day -33 was evaluated against this envelope and found to exceed the upper bound by more than 20 nT, a threshold well above the typical instrument noise level (±0.5–1 nT for Swarm VFM and ASM sensors). Although no formal hypothesis testing (e.g., t-test or ANOVA) was applied, the method incorporates a built-in statistical filter by comparing each day's magnetic profile to the ensemble mean and variability across a 35-day window. The anomaly's persistence, directional specificity (most prominent at the BN component), and isolation from adjacent time windows further support its statistical distinctiveness.

All three components of the recorded magnetic field are plotted in Figure 6. Among the three Swarm magnetic field components analyzed, the B_Val_N (Northward) component exhibits the most reliable and coherent anomaly. B_Val_E and B_Val_C also show less important anomalies according to Figure 5. The B_Val_N signal maintains a stable trend with a singular, well-defined anomaly that falls outside the characteristic curve method. This lends credibility to its interpretation as a potential pre-seismic magnetic precursor. Its presence in the Northward component, which is often sensitive to tectonic strain accumulation, aligns with previous findings that emphasize directional sensitivity in magnetic precursor detection (cf. De Santis et al., 2019). These results reinforce the value of Swarm satellite data in earthquake forecasting research, particularly when anomalies are isolated and component-specific.

The N-component anomaly stands out due to its clarity and isolation from background noise, particularly its distinct deviation from the characteristic curve method. Although the statistical significance of the N component of the magnetic field stands out due to its distinguished nature according to the characteristic curve method, the alignment of the anomalies in the two other components (E and C) emphasizes the anomalous nature of the observed data and strengthens its position as a strongly probable Chile 2014 earthquake precursor.

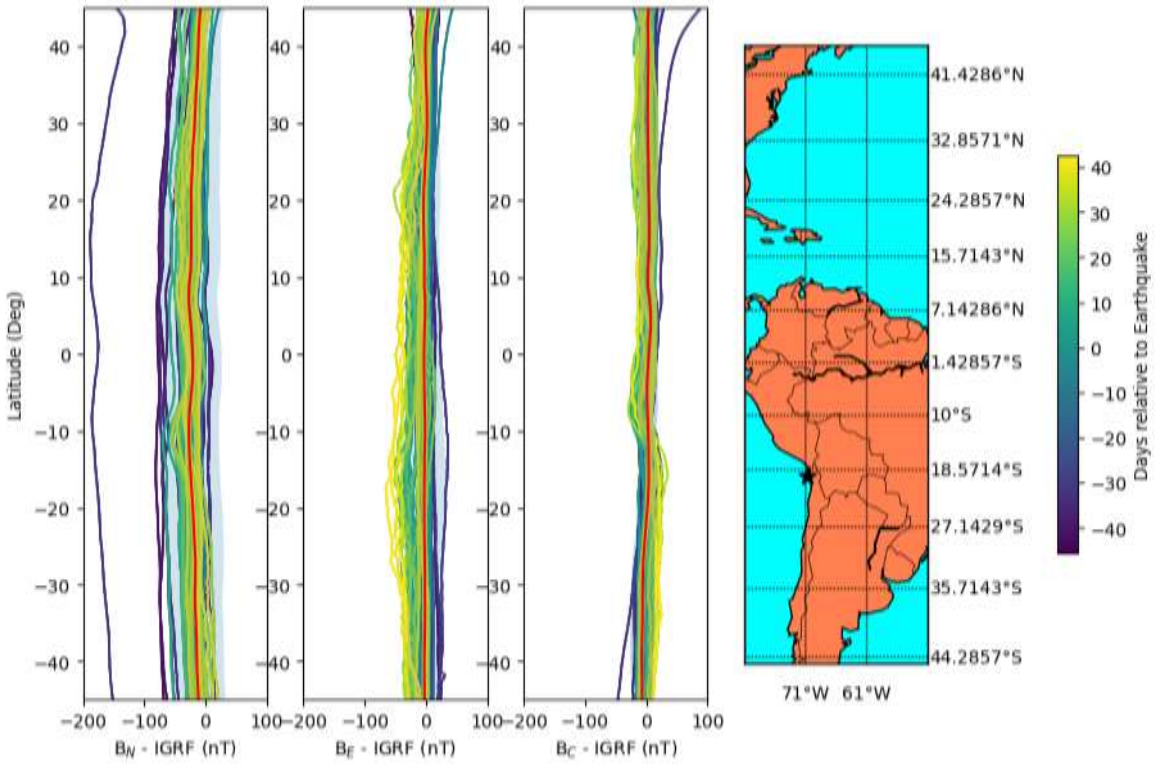

Figure 5. Characteristic curve analysis of Swarm satellite magnetic field data for earthquake precursor detection. Line plots show deviations from IGRF for BN, BE, and BC components versus latitude, with color-coded curves representing ±40 days around the earthquake. Shaded regions indicate ±2σ uncertainty bounds. A pronounced anomaly is observed in the BN component on day -33, exceeding the 2σ threshold, while less significant deviations are detected in the BE or BC components. The map panel shows the geographic region of data acquisition.

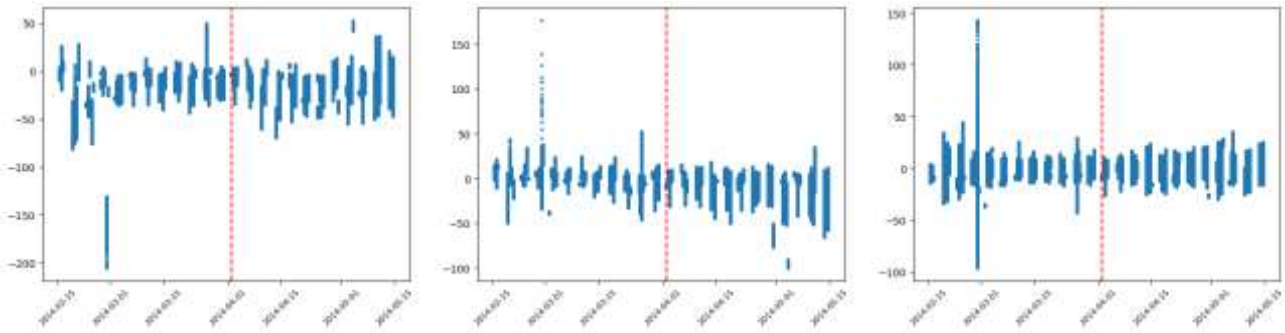

(a) (b) (c)

Figure 6. (a) B_Val_N: Northward component showing a clear anomaly 33 before April 1, 2014, Chile earthquake. (b) B_Val_E, Eastward component and (c) B_Val_C, Vertical component with spikes on the same date.

5. Discussion

The anomaly in the BN component may result from lithosphere-atmosphere-ionosphere coupling (LAIC) processes triggered by pre-seismic stress accumulation. Mechanisms include: Piezoelectric and electrokinetic effects in stressed rocks, which generate electric fields that propagate upward. These fields can modify ionospheric conductivity and current systems, especially the F-region, leading to detectable magnetic perturbations. At Swarm's orbital altitude (~460–530 km), such changes can manifest as localized magnetic deviations.

This study applied the characteristic curve method to Swarm satellite magnetic field data to investigate potential precursory signals preceding the 2014 Chile (Iquique) earthquake. A statistically significant anomaly was identified in the BN (northward) component 33 days before the event, exceeding the ±20 nT uncertainty bounds. This anomaly was weakly mirrored in the BE or BC components, suggesting directional specificity and reinforcing the hypothesis of a localized lithospheric-

ionospheric coupling mechanism.

In comparing our findings with those of De Santis et al. (2019), who reported a magnetic anomaly 27 days prior to the same earthquake using the MASS algorithm, it is important to contextualize the methodological and interpretive differences. Their study uses the data time derivative, while the present study works on the magnetic data itself. Using the time derivative is an effective method to detect the small-magnitude possible anomalies superimposing on highly variable data, such as the geomagnetic field, which is influenced by many factors, causing its magnitude to change within hundreds of nTs. However, in the case of SWARM satellite data, the variations in derivatives are so small that they fall within the range of the data uncertainty; thus, this method appears inefficient to be used as a tool for anomaly detection with this dataset.

Their analysis identified a disturbance in the Y component, which corresponds to the eastward direction in our coordinate system. However, when re-evaluated using the characteristic curve method with explicit uncertainty quantification, the reported anomaly falls within the ±20 nT or 2σ bounds and thus cannot be considered statistically robust. This discrepancy does not negate the value of their approach but highlights the sensitivity of precursor detection to the choice of statistical framework and component analysis. Rather than dismissing prior findings, our results refine the interpretation by emphasizing the importance of directional analysis and rigorous statistical thresholds.

Beyond statistical considerations, the physical basis for detecting magnetic anomalies as earthquake precursors warrants deeper exploration. The observed BN anomaly may reflect lithospheric stress accumulation that perturbs the local geomagnetic environment through a cascade of coupled processes. As tectonic stress builds in the crust, microfracturing and fluid migration can alter the conductivity and magnetic properties of rocks, generating electromagnetic emissions. These emissions may propagate upward, influencing atmospheric conductivity and triggering changes in the ionosphere. This lithosphere-atmosphere-ionosphere coupling (LAIC) mechanism has been proposed in several studies and is supported by observations of ionospheric anomalies preceding major seismic events.

At satellite altitude, Swarm instruments are sensitive to ionospheric and magnetospheric perturbations that may originate from lithospheric processes. The ionosphere, acting as a dynamic interface, can amplify or modulate these signals through interactions with atmospheric waves, electric fields, and plasma density variations. Additionally, the ionosphere itself is coupled to the magnetosphere, allowing localized disturbances to manifest as measurable magnetic field deviations in low-Earth orbit. The directional specificity of the BN anomaly suggests that the perturbation may be aligned with tectonic stress vectors or regional geomagnetic field orientation, further supporting a lithospheric origin.

The Swarm satellite constellation provides a unique vantage point for capturing these interactions due to its global coverage and high-resolution magnetic measurements. By filtering out long-term geomagnetic trends using the IGRF model and applying the characteristic curve method, we isolate short-term, localized anomalies that may serve as precursors. The mid-latitude location of the Chile earthquake also enhances detection reliability, as these regions are less affected by auroral and equatorial disturbances.

We analyzed similar time periods, e.g., two months before and three months after the studied 2-month time interval) in order to investigate the random effects. The plots can be found in Figure 7. There are some anomalies in the plots (for example, in the 3-month period before the study time span), but they are not apparently as strong as or comparable to the anomaly we detected 33 days before the earthquake. Furthermore, the plots showing the N, E and C component variations support this understanding that the most prominent anomaly is the one we observed before the earthquake. Ultimately, we acknowledge that this study is insufficient and in a position to add the anomaly to the earthquake. We are trying to figure out the anomaly at this stage and hopefully in future studies, we will go for earthquake precursor detection through several case studies like the present study.

To strengthen the interpretation of the

anomaly identified 33 days prior to the 2014 Chile earthquake, three sets of figures are presented. Each panel displays the deviation of the Swarm satellite magnetic field components (BN, BE, BC) from the IGRF model across geographic latitude and time. Figure 7a covers the period from December 1, 2013, to February 1, 2014 (approximately two months before the study window). Figure 7b **c**overs the period from April 1 to Jun 1, 2014 (approximately two months after the earthquake). Finally, Figure 7c corresponds to the study window from February 1 to April 1, 2014, and includes the anomaly discussed in the manuscript.

Across all panels, the BN component (northward magnetic field) is plotted alongside BE (eastward) and BC (vertical) components. In Figure 7c, a pronounced deviation in the BN component is observed around day -33, exceeding the $\pm 2\sigma$ uncertainty bounds. This anomaly is not mirrored in the earlier or later periods, where magnetic fluctuations remain within the expected envelope. The contrast between the three panels confirms that the anomaly in Figure 7c is temporally isolated and statistically significant, reinforcing its interpretation as a potential pre-seismic signal.

To assess the temporal and spatial uniqueness of the detected magnetic anomaly, we performed a rectangular search in the ISC Bulletin database covering the region bounded by latitudes $-70°$ to $50°$ and longitudes $-71°$ to $-61°$, spanning the period from 1 November 2013 to 1 July 2014. The search was constrained to events with magnitude ≥ 7. This query yielded only three major seismic events within the defined window:

-The Mw 8.2 Iquique earthquake on April 1, 2014 at 23:46 UTC

-A subsequent Mw 7.1 aftershock approximately 11 minutes later

-A third Mw 7.9 event on April 3, 2014

These events were localized within the same tectonic corridor off the northern Chilean coast, and their timing aligns precisely with the anomaly window identified in the Swarm satellite data. Given the absence of other major seismic activity in the region during the study period, it is reasonable to attribute the observed geomagnetic perturbations, particularly the BN component anomaly on day -33, to processes associated with these specific earthquakes. This strengthens the interpretation that the anomaly is not a random fluctuation but a localized, temporally isolated precursor signal. The spatial correlation between the epicentral region and the satellite's observational footprint further supports this conclusion, reinforcing the utility of Swarm data in identifying lithospheric-ionospheric coupling phenomena preceding large seismic events.

In summary, our findings demonstrate that satellite-based magnetic observations, when combined with rigorous statistical validation and physical modeling, offer a promising avenue for earthquake precursor research. The prominent anomaly detected in the BN component aligns with theoretical expectations of LAIC processes and underscores the importance of directional and temporal analysis. Future studies should expand this framework to additional seismic events and integrate complementary datasets, such as ionospheric electron density, atmospheric temperature profiles, and ground-based magnetometer readings, to further elucidate the mechanisms underlying lithosphere- ionosphere- magnetosphere interactions.

Geomagnetic indices such as Kp and Dst confirm that the anomaly observed 33 days before the 2014 Chile earthquake occurred during geomagnetically quiet conditions, supporting its interpretation as a potential seismic precursor rather than a space weather artifact. Hourly Kp index values for February 28, 2014, indicate geomagnetically quiet to moderate conditions during the observed magnetic anomaly window (Figure 7). The Kp index remained below storm thresholds ($Kp < 5$) throughout the day, with most intervals registering low activity ($Kp \leq 3$). These values confirm that the anomaly detected in Swarm satellite data occurred under quiet geomagnetic conditions, supporting its interpretation as a potential lithospheric precursor rather than a space weather artifact.

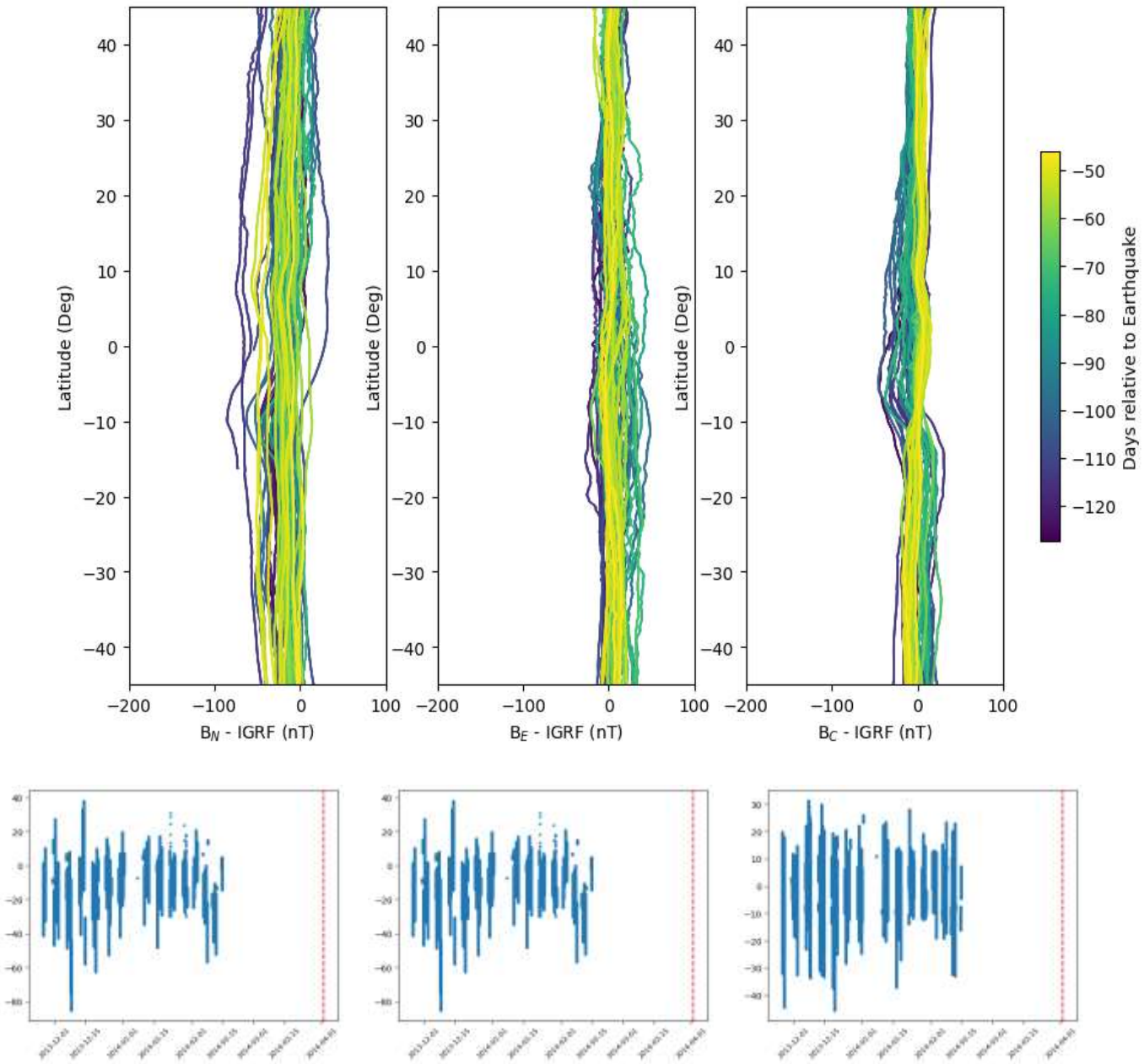
Latitude (Deg)
B_N - IGRF (nT)
B_E - IGRF (nT)
B_C - IGRF (nT)
Days relative to Earthquake
−50
−60
−70
−80
−90
−100
−110
−120

(a)

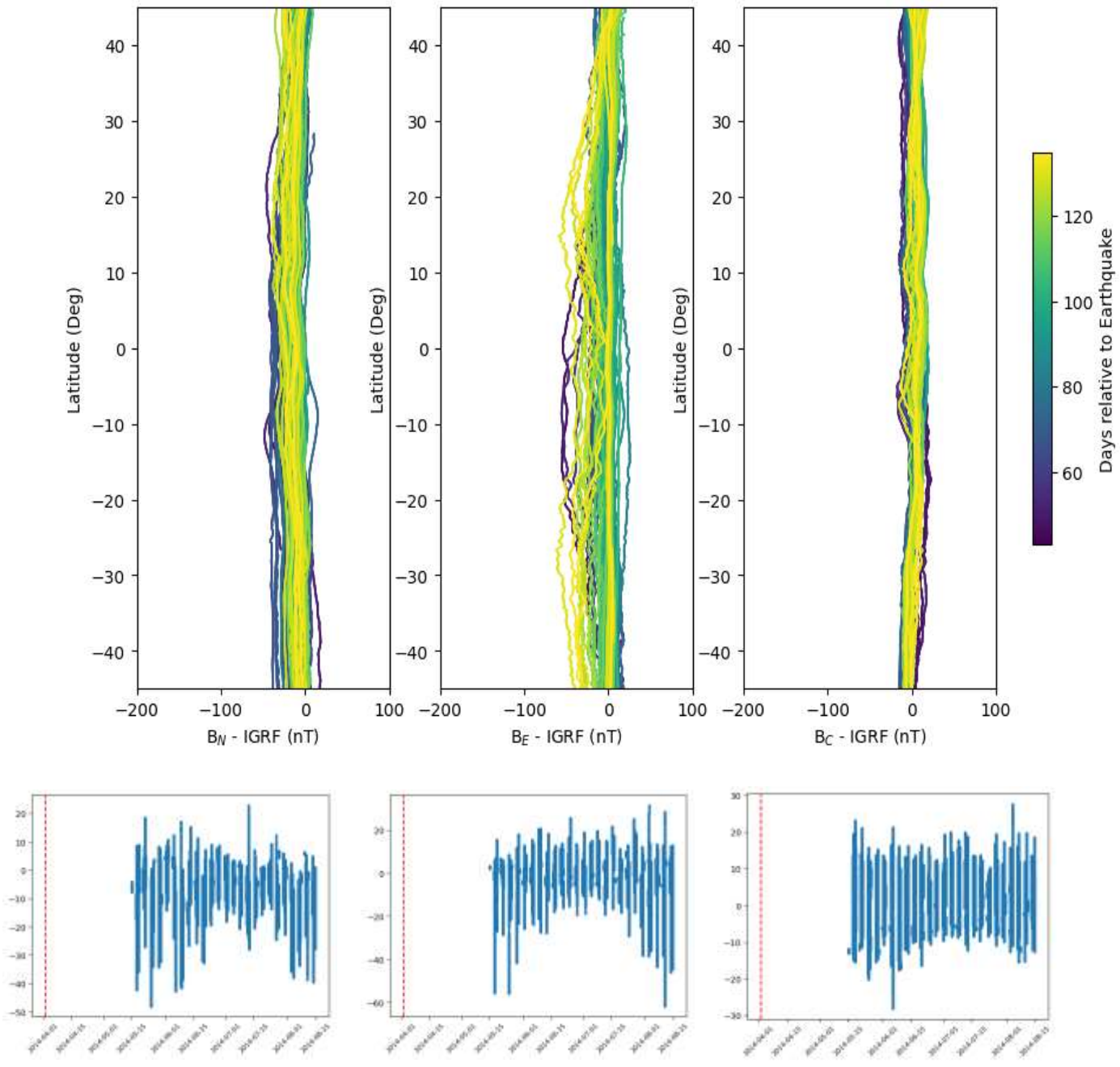
Latitude (Deg)
B_N - IGRF (nT)
B_E - IGRF (nT)
B_C - IGRF (nT)
Days relative to Earthquake

(b)

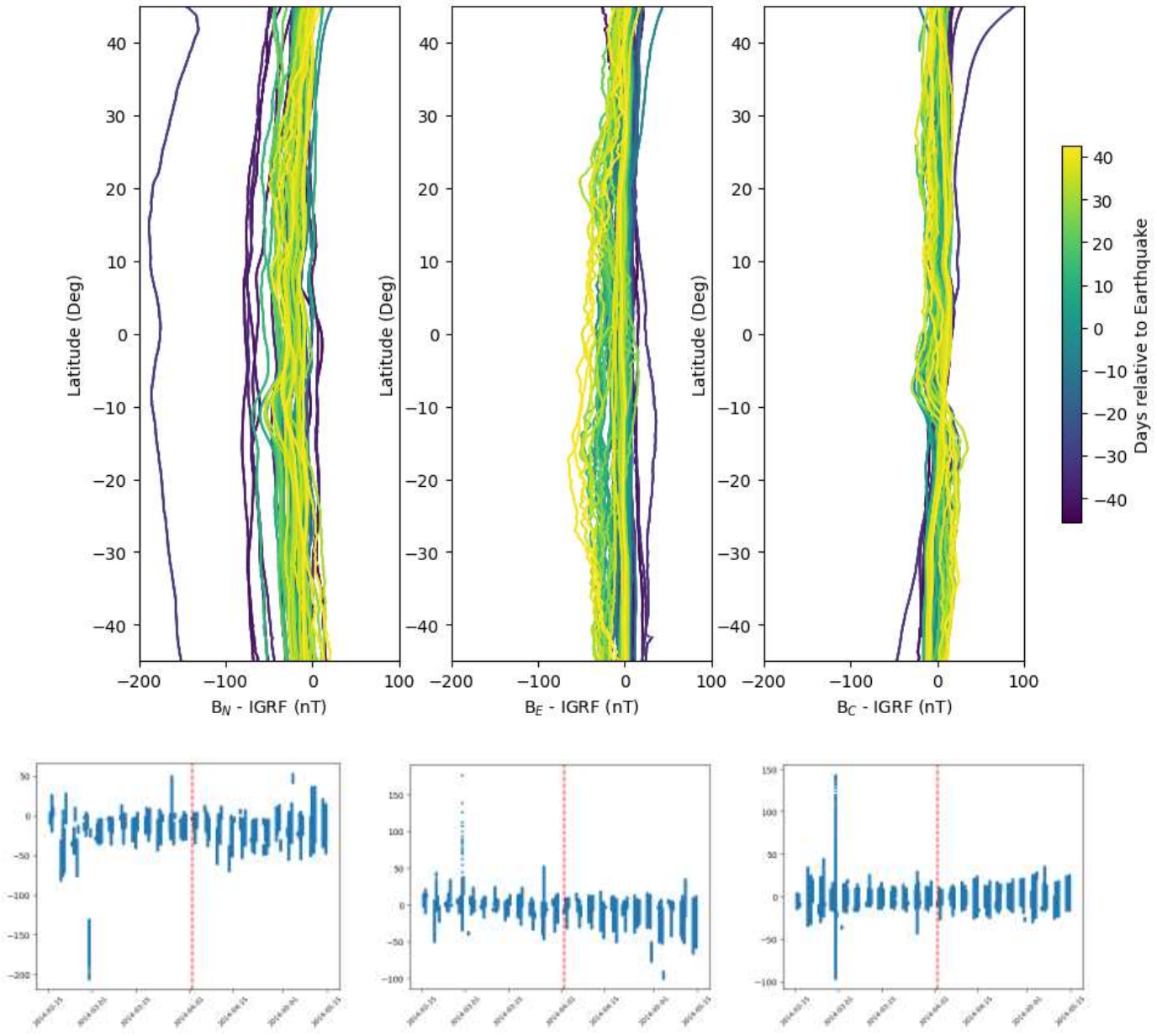

(c)

Figure 7. a) Swarm satellite magnetic field deviations (BN, BE, BC) from IGRF across latitude during the period December 1, 2013, to February 1, 2014. No statistically significant anomalies are observed in any component. This interval precedes the study window and serves as a control period. b) Swarm satellite magnetic field deviations (BN, BE, BC) from IGRF across latitude during the period April 1 to July 15, 2014. Magnetic field behavior remains within expected bounds, with no anomalies exceeding ±2σ. This interval follows the earthquake and supports the temporal specificity of the anomaly. c) Swarm satellite magnetic field deviations (BN, BE, BC) from IGRF across latitude during the study window, February 15 to April 1, 2014. A pronounced anomaly in the BN component is observed on day -33 relative to the earthquake, exceeding ±2σ bounds. This anomaly is statistically significant and temporally isolated, supporting its interpretation as a potential earthquake precursor.

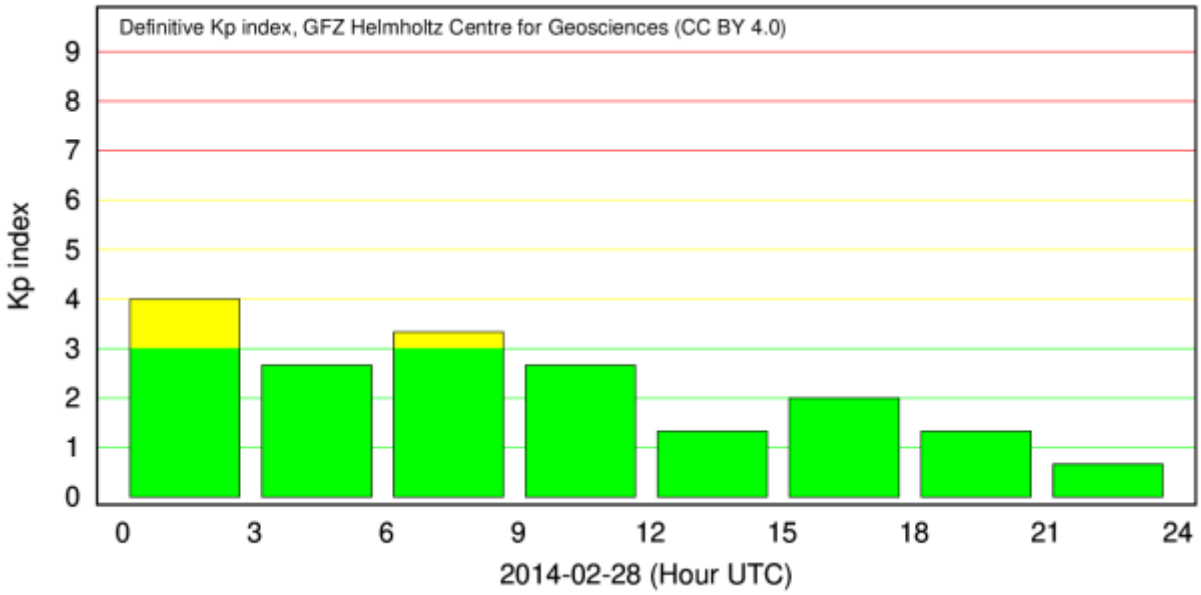

Figure 8. Kp index values on February 28, 2014 (day of observation of the geomagnetic anomaly in SWARM satellite data) confirm geomagnetically quiet conditions during the observed magnetic anomaly window.

6. Conclusion

This study applied the characteristic curve method to Swarm satellite magnetic field data to investigate potential precursory signals preceding the April 1, 2014, Mw 8.2 Chile earthquake. A statistically significant anomaly was identified in the northward (BN) magnetic component 33 days before the event, exceeding the ±20 nT uncertainty bounds. This anomaly was not mirrored in the eastward (BE) or vertical (BC) components, indicating directional specificity and reinforcing the hypothesis of a localized lithospheric-ionospheric coupling mechanism.

To further validate the anomaly's uniqueness, supplementary figures were analyzed from two control intervals: three months before and three months after the study window. These comparative panels revealed no comparable deviations in magnetic components during the control periods, confirming that the BN anomaly observed during the study window is temporally isolated and statistically distinct. Among all three figure sets, the anomaly in the BN component during the February 15 to April 1 interval stands out as the most prominent, both in amplitude and persistence. The statistical robustness of the anomaly was assessed using a sliding window approach that generated envelopes of median ± standard deviation across latitudinal profiles. The anomaly on day -33 exceeded the upper bound by more than 20 nT, well beyond the typical instrument noise level of Swarm's magnetometers. This built-in statistical filter, combined with directional analysis and temporal isolation, strengthens the interpretation of the anomaly as a genuine pre-seismic signal. In comparison with prior studies, such as De Santis et al. (2019), which reported a magnetic anomaly 27 days before the same earthquake using the MASS algorithm, our findings refine the interpretation by emphasizing the importance of component-wise analysis and rigorous uncertainty quantification. While their method relied on time derivatives, our approach directly analyzes magnetic field values, which proved more effective for Swarm data, given its low derivative variability.

Overall, the integration of the characteristic curve method, IGRF subtraction, and comparative temporal analysis demonstrates a reliable framework for identifying magnetic precursors to large earthquakes. The results support the broader hypothesis that lithospheric stress accumulation can manifest as detectable magnetic anomalies via lithosphere-atmosphere-ionosphere coupling processes. Future research should extend this methodology to additional seismic events and incorporate complementary ionospheric and atmospheric datasets to further elucidate the mechanisms underlying electromagnetic earthquake precursors.

References

Akhoondzadeh, M. (2025). Predicting the magnitude and time of an upcoming strong earthquake using satellite-based seismo-LAI anomalies. *Geomagnetism and Aeronomy*. https://doi.org/10.1134/S0016793225600043

Akhoondzadeh, M., De Santis, A., Marchetti, D. & Piscini, A. (2018). Multi-precursors analysis associated with the powerful Ecuador (Mw = 7.8) earthquake of 16 April 2016 using Swarm satellite data in conjunction with other multi-platform observations. *Advances in Space Research*, 61(1), 248–263. https://doi.org/10.1016/j.asr.2017.09.021.

Akhoondzadeh, M., De Santis, A., Marchetti, D., & Wang, T. (2022). Developing a deep learning-based detector of magnetic, Ne, Te and TEC anomalies from Swarm satellites: The case of Mw 7.1 2021 Japan earthquake. Remote Sensing, 14(7), 1582. https://doi.org/10.3390/rs14071582

Christodoulou, P., Bi, Y. & Wilkie, G. (2019). Detection of geomagnetic anomalies using Swarm satellite data and machine learning techniques. *Remote Sensing*, 11(3), 345. https://doi.org/10.3390/rs11030345.

Conti, L., Picozza, P., & Sotgiu, A. (2021). A critical review of ground-based observations of earthquake precursors. *Frontiers in Earth Science*, 9, 676766. https://doi.org/10.3389/feart.2021.676766 (Note: This paper is paired with a companion article on satellite-based observations in the same volume.)

Conti, L., Picozza, P., & Sotgiu, A. (2021). A critical review of ground-based observations of earthquake precursors. *Frontiers in Earth Science*, 9, Article 676766. https://doi.org/10.3389/feart.2021.676766

De Santis, A., Marchetti D. & Pavón-Carrasco, F. J., (2019). Precursory worldwide signatures of earthquake occurrences on Swarm satellite data. *Scientific Reports*, 9, 14022. https://doi.org/10.1038/s41598-019-56599-1.

De Santis, A., Marchetti, D., & Pavón-Carrasco, F. J. (2019). Precursory worldwide signatures of earthquake occurrences on Swarm satellite data. *Scientific Reports*, 9, Article 14022. https://doi.org/10.1038/s41598-019-56599-1

De Santis, A., Marchetti, D., Pavón-Carrasco, F. J., Cianchini, G. & Perrone, L. (2017). Potential ionospheric precursors of the 2015 Nepal earthquake detected by satellite data. *Annals of Geophysics*, 60(1), S0101. https://doi.org/10.4401/ag-7386.

Dobrovolsky, I.P., Zubkov, S.I. & Miachkin, V.I. (1979). Estimation of the size of earthquake preparation zones. PAGEOPH 117, 1025–1044, https://doi.org/10.1007/BF00876083.

European Space Agency. (2019). Swarm Level 1b Processor Algorithms (SW-RS-DSC-SY-0002, Issue 6.11). Technical University of Denmark.

European Space Agency. (2019). Swarm Level 1b Processor Algorithms (SW-RS-DSC-SY-0002, Issue 6.11). https://earth.esa.int/eogateway/documents/20142/37627/swarm-level-1b-processor-algorithms.pdf

European Space Agency. (n.d.). Swarm - Earth Online. Retrieved from https://earth.esa.int/eogateway.

Fenoglio, M. A., Johnston, M. J. S., & Byerlee, J. D. (1995). Magnetic and electric fields associated with changes in high pore pressure in fault zones: Application to the Loma Prieta ULF emissions. *Journal of Geophysical Research: Solid Earth*, 100(B7), 12951–12958. https://doi.org/10.1029/95JB00076

Friis-Christensen, E., Lühr, H. & Hulot, G. (2006). Swarm: A constellation to study the Earth's magnetic field. *Earth, Planets and Space*, 58(4), 351–358. https://doi.org/10.1186/BF03351933.

Friis-Christensen, E., Lühr, H., & Hulot, G. (2006). Swarm: A constellation to study the Earth's magnetic field. *Earth, Planets and Space*, 58(4), 351–358. https://doi.org/10.1186/BF03351933

Ghamry, E., El-Gohary, M. & Abd El-Aziz, M. (2021). Detection of geomagnetic anomalies associated with earthquakes using Swarm satellite data. *Journal of Geophysical Research: Space Physics*, 126(4), e2020JA028885. https://doi.org/10.1029/2020JA028885.

Hegy, M. (2025). Detecting earthquake precursors using Swarm satellite data. In

V. Demyanov (Ed.), Satellite Systems for Navigation and Geosciences [Working Title]. IntechOpen. https://doi.org/10.5772/intechopen.1011315

IAGA. (n.d.). International Association of Geomagnetism and Aeronomy. https://iaga-aiga.org/

Jackson, A. (2015). Earth's magnetic field and Swarm. In G. Hulot et al. (Eds.), Earth's Magnetic Field: Understanding Geomagnetic Sources from the Earth's Interior to the Sun (pp. 1–20). Springer. https://doi.org/10.1007/978-3-642-32135-3_1.

Léger, J.-M., Jager, T., Bertrand, F., Hulot, G., Brocco, L., Vigneron, P., ... & Fratter, I. (2015). In-flight performance of the Absolute Scalar Magnetometer vector mode on board the Swarm satellites. *Earth, Planets and Space*, 67(1), 57. https://doi.org/10.1186/s40623-015-0231-1.

Liu, J.-Y. T., Shen, X., Chang, F.-Y., Chen, Y.-I., Sun, Y.-Y., Chen, C.-H., ... Wang, Q. (2024). Spatial analyses on pre-earthquake ionospheric anomalies and magnetic storms observed by China seismo-electromagnetic satellite in August 2018. *Geoscience Letters*, 11(4). https://doi.org/10.1186/s40562-024-00320-2

Pavlovic, M., Bi, Y. & Nicholl, P. (2021). Extracting anomalous pre-earthquake signatures from Swarm satellite data using EOF and PCA analysis. In Knowledge Science, Engineering and Management (pp. 394–405). *Springer*. https://doi.org/10.1007/978-3-030-82147-0_32.

Pulinets, S., & Ouzounov, D. (2011). Lithosphere–atmosphere–ionosphere coupling (LAIC) model, a unified concept for earthquake precursors validation. *Journal of Asian Earth Sciences*, 41(4–5), 371–382. https://doi.org/10.1016/j.jseaes.2010.03.005

Richter, C. F. (1958). Elementary Seismology. W.H. Freeman and Company.

Sasai, Y. (1991). Application of the piezomagnetic effect to the investigation of the stress state of the crust. *Journal of Geomagnetism and Geoelectricity*, 43(Supplement), 55–78. https://doi.org/10.5636/jgg.43.Supplement_55

Taherinya, H., & Pourbeyranvand, S. (2021). Analysis of geomagnetic data as earthquake precursors for the September 2018 Mw 6.6 Japan earthquake. *New Findings in Applied Geology*, 15(29), 135–148. [In Persian].

Zhu, X., De Santis, A., Marchetti, D. & Akhoondzadeh, M. (2019). Analysis of Swarm satellite magnetic data before the 2016 Ecuador earthquake using non-negative matrix factorization. *Remote Sensing*, 11(5), 567. https://doi.org/10.3390/rs11050567.